Resonant Dephasing in the Electronic Mach-Zehnder Interferometer

Eugene V. Sukhorukov[1] and Vadim V. Cheianov[2]

[1]Départment de Physique Théorique, Université de Genève, CH-1211 Genève 4, Switzerland
[2]Physics Department, Lancaster University, Lancaster, LA1 4YB, UK

(Received 22 September 2006; published 10 October 2007)

We address the recently observed unexpected behavior of Aharonov-Bohm oscillations in the electronic Mach-Zehnder interferometer that was realized experimentally in a quantum Hall system [I. Neder *et al.*, Phys. Rev. Lett. **96**, 016804 (2006)]. We argue that the measured lobe structure in the visibility of oscillations and the phase rigidity result from a strong long-range interaction between two adjacent counterpropagating edge states, which leads to a resonant scattering of plasmons. The visibility and phase shift, which we express in terms of the transmission coefficient for plasmons, can be used for the tomography of edge states.

DOI: 10.1103/PhysRevLett.99.156801 PACS numbers: 73.23.−b, 03.65.Yz, 85.35.Ds

Quantum interference effects, particularly the Aharonov-Bohm (AB) effect [1], and their suppression due to interactions [2] have always been a central subject of mesoscopic physics, and by now are thoroughly investigated. However, recent experiments on the AB effect in Mach-Zehnder (MZ) [3,4] and Fabry-Perot–type [5] interferometers, which utilize quantum Hall edge states [6] as one-dimensional conductors, have posed a number of puzzles indicating that the physics of edge states is not yet well understood [7]. For instance the lobe-type pattern in the visibility of AB oscillations as a function of voltage bias, as well as the rigidity of the phase of oscillations followed by abrupt jumps by π, observed in Ref. [3], cannot be explained within the single-particle formalism [8] that is supposed to describe edge states at integer filling factor [9].

Indeed, according to a single-particle picture, the electron edge states propagate as plane waves with the group velocity v_F at Fermi level. They are transmitted through the MZ interferometer (see Fig. 1) at the left and right quantum point contacts (QPCs) with amplitudes t_L and t_R, respectively. In the case of low transmission, two amplitudes add so that the total transmission probability $T \propto |t_L|^2 + |t_R|^2 + 2|t_L t_R| \cos(\varphi_{\rm AB} + \Delta\mu\Delta x/v_F)$ oscillates as a function of the AB phase $\varphi_{\rm AB}$ and bias $\Delta\mu$, where Δx is the length difference between two interfering paths of the interferometer. The AB oscillations may be seen in the differential conductance $G = dI/d\Delta\mu$, which is given by the Landauer-Büttiker formula [8], $G = T/2\pi$. The degree of coherence is quantified by the visibility of AB oscillations $V_{\rm AB} = (G_{\rm max} - G_{\rm min})/(G_{\rm max} + G_{\rm min})$, which for low transmission acquires the simple form

$$V_{\rm AB}^{(0)} = 2|t_L t_R|/(|t_L|^2 + |t_R|^2); \quad (1)$$

i.e., it is independent of bias. Moreover, the phase shift of AB oscillations is just a linear function of bias; $\Delta\varphi_{\rm AB} = \Delta\mu\Delta x/v_F$.

Dephasing in ballistic mesoscopic rings was reported in Ref. [10] and theoretically addressed in Ref. [11]. Since the first experiment on an electronic MZ interferometer [4], several theoretical models of dephasing in this particular system have been proposed, including classical fluctuating field [12] and dephasing probe [13] models. However, the unusual dephasing of AB oscillations in Ref. [3] (also see [14]) seems to arise from a specific interaction at the edge of a quantum Hall system.

In this Letter we propose a model which may explain the unusual AB effect. We note that an important feature of the MZ setup [3] is the existence of a counterpropagating edge state (labeled as ϕ_3 in Fig. 1), which closely approaches the edge state forming the upper arm of the interferometer (labeled as ϕ_2 in Fig. 1) and strongly interacts with it [15]. Being localized inside a finite interval of the length L, the interaction leads to a resonant scattering of collective charge excitations (plasmons), which carry away the phase information. As a result, AB oscillations vanish at certain

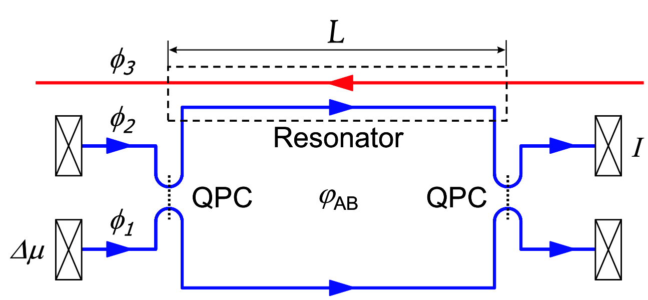

FIG. 1 (color online). Schematic representation of the electronic Mach-Zehnder interferometer experimentally realized in Ref. [3]. Two edge states (blue lines, ϕ_1 and ϕ_2), which propagate from left to right, are coupled via two quantum point contacts and form the Aharonov-Bohm loop. The bias $\Delta\mu$ applied to one of the source Ohmic contacts causes the current I to flow around the loop, so that the differential conductance $G = dI/d\Delta\mu$ oscillates as a function of the phase $\varphi_{\rm AB}$. The specific property of the setup in Ref. [3] is that the third counterpropagating edge state (red line, ϕ_3) closely approaches the upper branch of the MZ interferometer (inside the resonator shown by a dashed box) and strongly interacts with it.

values of bias $\Delta\mu$ (see Fig. 2), where the AB phase jumps by π. We found an important relation between the transmission coefficient of plasmons and the visibility of AB oscillation, Eqs. (5) and (11), which opens a possibility for the tomography of the edge state interactions.

Model of a Mach-Zehnder interferometer.—To describe quantum Hall edges at filling factor $\nu = 1$, we apply the chiral Luttinger liquid model [9,16] and write the Hamiltonian as $H = (v_F/4\pi)\sum_\alpha \int dx[\nabla\phi_\alpha(x)]^2 + H_{\rm int}$. The bosonic fields ϕ_α, $\alpha = 1, 2, 3$, describe low-energy collective charge excitations at the edges; $\rho_\alpha(x) = (1/2\pi)\nabla\phi_\alpha(x)$. They satisfy the commutation relations: $[\phi_\alpha(x), \phi_\alpha(y)] = \pm i\pi\,\mathrm{sgn}(x-y)$, where the minus sign stands for the counterpropagating field ϕ_3. Details of the interaction $H_{\rm int}$ are not exactly known. Here we assume a general density-density interaction: $H_{\rm int} = (1/2)\sum_{\alpha\beta} dxdyU_{\alpha\beta}(x,y)\rho_\alpha(x)\rho_\beta(y)$.

We note that electron-electron interaction within one edge, while generally leading to a smooth suppression of the visibility [17] as a function of $\Delta\mu$, cannot explain the lobe structure observed in Ref. [3]. We therefore further assume that only the elements U_{23} and $U_{22} = U_{33}$ inside the resonator are nonzero. Going over to the canonical variable $\phi = (\phi_2 + \phi_3)/2$ and its dual variable $\theta = (\phi_3 - \phi_2)/2$, such that $[\phi(x), \nabla\theta(y)] = i\pi\delta(x-y)$, we obtain the final Hamiltonian $H = (v/4\pi)\times \int dx[\nabla\phi_1(x)]^2 + H_{\rm LL}$, where the important part,

$$H_{\rm LL} = \frac{v_F}{2\pi}\int dx[(\nabla\phi)^2 + (\nabla\theta)^2] + \iint\frac{dxdy}{4\pi^2} \times[U(x,y)\nabla\phi(x)\nabla\phi(y) + V(x,y)\nabla\theta(x)\nabla\theta(y)], \tag{2}$$

takes into account the interaction, $U \equiv U_{22} + U_{23}$, $V \equiv U_{22} - U_{23}$, at the resonator.

In the experiment [3], two point contacts located at x_ℓ, $\ell = L, R$, mix the edge states and allow interference between them. This can be described by the tunneling Hamiltonian [18]

$$H_T = A + A^\dagger, \qquad A = A_L + A_R, \tag{3a}$$

$$A_\ell = t_\ell\psi_2^\dagger(x_\ell)\psi_1(x_\ell), \qquad \ell = L, R, \tag{3b}$$

where ψ_1 and ψ_2 are electron operators, and the tunneling amplitudes t_ℓ depend on the Aharonov-Bohm phase $\varphi_{\rm AB}$.

Visibility of Aharonov-Bohm oscillations.—We will investigate interference effects in the tunneling current $I = i(A - A^\dagger)$; see Fig. 1. To the lowest order in tunneling amplitudes t_ℓ its expectation value is given by $I = \int dt\langle[A^\dagger(t), A(0)]\rangle$ [19], where the average is taken with respect to the ground state of the system biased by the potential difference $\Delta\mu$. Taking into account Eqs. (3), we write the total current as a sum of three terms: $I = I_L + I_R + I_{LR}$, where two terms $I_\ell = \int dt\langle[A_\ell^\dagger(t), A_\ell(0)]\rangle$ are direct contributions of two point contacts, and $I_{\rm LR} = \int dt\langle[A_L^\dagger(t), A_R(0)]\rangle + \text{c.c.}$ is the interference term that contains the AB phase.

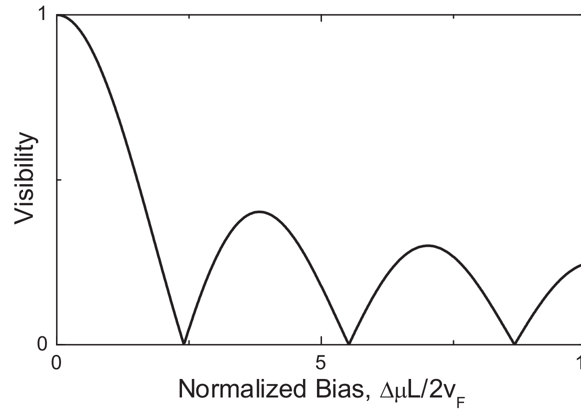

FIG. 2. In the case of a long-range interaction of counterpropagating edge states at the resonator of the length L (see Fig. 1), the visibility of Aharonov-Bohm oscillations varies as a function of the normalized bias, $\Delta\mu L/2v_F$, in a lobelike manner. The phase of AB oscillations (not shown) stays constant at the lobes and changes abruptly by π at zeros of the visibility. The visibility is plotted here for the simplified capacitive coupling model, Eq. (14), with $T_L = T_R$.

Next, we recall that in our model the interaction is effectively present only at the resonator between points x_L and x_R. There are two important consequences of this. First, the interaction cannot affect direct contributions I_L and I_R. Therefore, we readily obtain the conductances for noninteracting electrons: $dI_\ell/d\Delta\mu = G_\ell = 2\pi n_F^2|t_\ell|^2$, where n_F is the density of states at the Fermi level. And second, the interference term, $G_{LR} = n_F t_L t_R \times \exp(i\Delta\mu\Delta x/v_F)\mathcal{G}_{\Delta\mu} + \text{c.c.}$, still depends on the interaction via the Fourier transform $\mathcal{G}_{\Delta\mu} = v_F^{-1}\int dX \times \exp[i(\Delta\mu/v_F)X]\mathcal{G}(X)$ of the electronic correlator

$$\mathcal{G}(X) = \langle\psi_2(x_L, t)\psi_2^\dagger(x_R)\rangle, \tag{4}$$

which, however, depends on coordinates only via the combination $X \equiv x_R - x_L + v_F t$. Thus we obtain an important result for the visibility of AB oscillations and for the AB phase shift:

$$V_{\rm AB}/V_{\rm AB}^{(0)} = (1/2\pi n_F)|\mathcal{G}_{\Delta\mu}|, \tag{5a}$$

$$\Delta\varphi_{\rm AB} = \Delta\mu\Delta x/v_F + \arg(\mathcal{G}_{\Delta\mu}), \tag{5b}$$

where $V_{\rm AB}^{(0)}$ is the visibility in the absence of interaction; see Eq. (1).

Electron correlation function.—As a next step, we quantize plasmons, taking into account inhomogeneous interaction. The Hamiltonian (2) generates two coupled equations of motion for fields ϕ and θ. We choose periodic boundary conditions on the spatial interval of the length W, which in the end is taken to infinity. Then the equations of motion may be solved in terms of an infinite set $\{\Phi_n, \Theta_n\}$ of mutually orthogonal eigenfunctions that satisfy equations

$$\omega_n\Phi_n + v_F\nabla\Theta_n = -(2\pi)^{-1}\int dy V(x,y)\nabla\Theta_n(y), \quad (6a)$$

$$\omega_n\Theta_n - v_F\nabla\Phi_n = (2\pi)^{-1}\int dy U(x,y)\nabla\Phi_n(y) \quad (6b)$$

and can be chosen to be real and normalized as follows:

$$\int_0^W dx\Phi_n(x)\nabla\Theta_m(x) = -\omega_n\delta_{nm}. \quad (7)$$

The solutions then read

$$\phi(x,t) = \sum_n\sqrt{\frac{\pi}{2\omega_n}}\Phi_n(x)(a_n e^{-i\omega_n t} + a_n^\dagger e^{i\omega_n t}), \quad (8a)$$

$$\theta(x,t) = i\sum_n\sqrt{\frac{\pi}{2\omega_n}}\Theta_n(x)(a_n e^{-i\omega_n t} - a_n^\dagger e^{i\omega_n t}), \quad (8b)$$

where the plasmon operators a_n satisfy the commutation relations $[a_n, a_m^\dagger] = \delta_{nm}$ and diagonalize the Hamiltonian: $H_{LL} = \sum_n \omega_n a_n^\dagger a_n$.

Proceeding with the bosonization of the electron operators, we write $\psi_2 \propto \exp[i(\phi - \theta)]$, where the normalization prefactor is determined by the ultraviolet cutoff [16]. In the zero-temperature case considered here the evaluation of the correlation function $\mathcal{G}(X)$ amounts to normal ordering of the product $\psi_2(x_L, t)\psi_2^\dagger(x_R)$, taking into account Eqs. (8). We finally obtain the following result:

$$\log\mathcal{G} = -\sum_n\frac{\pi}{4\omega_n}\{|F_n(x_L)|^2 + |F_n(x_R)|^2 - 2F_n^*(x_L)F_n(x_R)e^{-i\omega_n t}\}, \quad (9)$$

where $F_n(x) = \Phi_n(x) + i\Theta_n(x)$.

Scattering of plasmons.—We note that the result (9) holds for arbitrary potentials U and V. However, in our model the interaction is localized between points x_L and x_R; therefore, the correlator (9) can be expressed in terms of the scattering properties of plasmons. Indeed, in an open system, the differential Eqs. (6) describe the scattering of incoming plane waves with continuous spectrum $\omega = v_F k > 0$ to outgoing plane waves. The scattering matrix is symmetric; therefore, quite generally we can write for the transmission coefficient $\mathcal{T} = |\mathcal{T}|e^{i\varphi}$ and for the reflection coefficients $\mathcal{R} = i|\mathcal{R}|e^{i(\varphi+\delta)}$ and $\mathcal{R}' = i|\mathcal{R}|e^{i(\varphi-\delta)}$, where φ and δ are scattering phases. Imposing now the periodic boundary condition on the interval $[0, W]$, we obtain a discrete set of eigenfunctions $\{\Phi_n, \Theta_n\}$, $n = 0, \pm 1, \dots$, which take the following form outside the scattering region:

$$\Phi_n(x) = \sqrt{\frac{2v_F}{W}} \times \begin{cases} \sin[k_n x - \frac{1}{2}(k_n W + \delta)], & n > 0, \\ \cos[k_n x - \frac{1}{2}(k_n W + \delta)], & n < 0, \end{cases} \quad (10)$$

and $\Theta_n(x) = \Phi_{-n}(x)$. They are normalized according to Eq. (7), and the spectrum is given by $k_n W = |2\pi n + \arccos|\mathcal{T}| - \varphi|$.

Substituting now Φ_n and Θ_n from Eq. (10) into Eq. (9) and taking the limit $W \to \infty$, we finally express the correlation function of electrons in terms of the transmission coefficient $\mathcal{T}$ for plasmons:

$$\log\mathcal{G}(X) = -\int_0^\infty\frac{dk}{k}[1 - \mathcal{T}^*(k)e^{-iXk}], \quad (11)$$

where, we remind, $X \equiv x_R - x_L + v_F t$. This equation together with Eqs. (5) is one of the central results of our paper. In the noninteracting case the transmission is perfect, $\mathcal{T} = 1$, and Eq. (11) generates the correlator $\mathcal{G} = -iv_F n_F/(X - i0)$ for free fermions. One obtains $|\mathcal{G}_{\Delta\mu}| = 2\pi n_F$, which implies [see Eqs. (5)] that the transport is coherent for arbitrary bias $\Delta\mu$. Conversely, in the case of nonzero interaction $\mathcal{T} \to 0$ for large k, the correlator $\mathcal{G}$ becomes independent of t, and the visibility V_{AB} vanishes for large bias $\Delta\mu$. Next, we consider a simple and natural model of a long-range interaction, which qualitatively reproduces the puzzling results of the experiment [3].

Long-range interaction model.—We assume capacitive coupling between edge states: $H_{\mathrm{int}} = Q^2/2C$, where $Q = \int_0^L dx(\rho_2 + \rho_3)$ is the total charge in the interaction region. Then $U = 2/C$ inside the interval $[0, L]$, while $V = 0$. The Eqs. (6) are straightforward to solve, and we obtain the transmission coefficient: $\mathcal{T} = 1 + (1/2)|D|^2/(D + i\pi\omega C)$, where $D = e^{ikL} - 1$.

We are interested in the first few resonances; therefore $kL \sim 1$. Then the second term in the denominator of $\mathcal{T}$ is of the order of v_F/e^2, i.e., the inverse interaction constant. In the quantum Hall system of [3] this value is much smaller than 1, so the second term in the denominator can be neglected, and we arrive at

$$\mathcal{T} = (1 + e^{-ikL})/2. \quad (12)$$

It is quite remarkable that the interaction constant drops from the final result, leading to the universality which will be addressed below.

The evaluation of the integral (11) is now straightforward, and we obtain the electron correlator

$$\mathcal{G}(X) = -iv_F n_F[(X - i0)(X - L - i0)]^{-1/2}. \quad (13)$$

Evaluating further the Fourier transform of $\mathcal{G}$, we find that $\mathcal{G}_{\Delta\mu} = 2\pi n_F \exp(i\Delta\mu L/2v_F)J_0(\Delta\mu L/2v_F)$, where J_0 is the zero-order Bessel function. Finally, using Eqs. (5) we obtain that (see Fig. 2)

$$V_{\mathrm{AB}}/V_{\mathrm{AB}}^{(0)} = |J_0(\Delta\mu L/2v_F)|, \quad (14)$$

while $\varphi_{\mathrm{AB}}(\Delta\mu)$ exhibits π jumps at the zeros of the Bessel function, in full agreement with the experiment [3]. The characteristic L dependence of the position of zeros of the visibility suggests that our theory may be experimentally verified by changing the length L of the resonator.

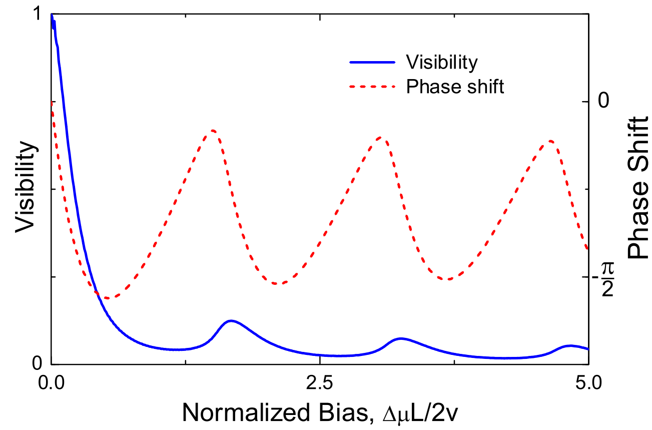

FIG. 3 (color online). The visibility for the case of a short-range interaction inside the resonator (Luttinger constant $K = 0.1$) is plotted versus bias normalized to the interaction dependent group velocity v of plasmons.

The key feature of the model is the presence of strong jumps in the potential U at the points $x = 0$ and $x = L$. The system compensates this effect by adjusting $\Phi(0) = \Phi(L)$, which immediately gives $\mathcal{T} e^{ikL} = 1 + \mathcal{R}$, and $\mathcal{T} = e^{-ikL} + \mathcal{R}' e^{ikL}$, independent of details of the interaction. Solving these equations we obtain $\mathcal{T} = \cos\gamma e^{i(\gamma - kL)}$, where the phase γ depends on the interaction. In our capacitive model U is constant, and 2γ is equal to the phase kL, accumulated between $x = 0$ and $x = L$, which leads to the result (12). The phase γ will increase if the realistic repulsive interaction is taken into account. However, this should merely shift zeros of the visibility downward, as compared to zeros of the Bessel function.

Short-range interaction model.—To complete our analysis, we investigate the case of short-range interactions at the edge and therefore write $U = 2\pi U_0 \delta(x - y)$ and $V = 2\pi V_0 \delta(x - y)$. Then the Hamiltonian acquires the standard form [16] $H_{\rm LL} = (1/2\pi) \int dx[(v/K)(\nabla\phi)^2 + vK(\nabla\theta)^2]$. The jump in the group velocity v and the Luttinger constant K at the points $x = 0$ and $x = L$ lead to resonant scattering of plasmons. The result for the electronic correlator may be presented as follows:

$$\mathcal{G} = -iv_F n_F \prod_{n=0}^{\infty} [X + X_n - i0]^{-\alpha_n}, \qquad (15)$$

where $X_n = [(2n + 1)(v_F/v) - 1]L$, and $\alpha_n = 4K/(K + 1)^2 \times [(K - 1)/(K + 1)]^{2n}$. The infinite product in (15) is due to multiple scattering at the ends of the resonator and X_n are the lengths of corresponding paths. The result of the numerical evaluation of the Fourier transform for $\mathcal{G}_{\Delta\mu}$ is shown in Fig. 3. Note that the lobe-type structure in the visibility is absent and the phase shift develops smooth oscillations. This behavior disagrees with experimental findings.

To summarize, we have demonstrated that the lobe structure and phase slips observed in Ref. [3] provide evidence of strong long-range interaction between quantum Hall edge states. By comparing two different models of edge states, we have demonstrated strong sensitivity of AB oscillations to the character of the interaction. This suggests that AB interferometry can be used as a powerful tool for the tomography of interactions at the quantum Hall edge and possibly in other systems.

We acknowledge support from the Swiss NSF. V. C. is grateful for the hospitality of workshop COQUSY06 at the MPI, Dresden.

[1] Y. Aharonov and D. Bohm, Phys. Rev. **115**, 485 (1959).
[2] B. L. Altshuler, A. G. Aronov, and D. E. Khmelnitsky, J. Phys. C **15**, 7367 (1982).
[3] I. Neder *et al.*, Phys. Rev. Lett. **96**, 016804 (2006).
[4] Y. Ji *et al.*, Nature (London) **422**, 415 (2003).
[5] F. E. Camino, W. Zhou, and V. J. Goldman, Phys. Rev. B **72**, 075342 (2005).
[6] *The Quantum Hall Effect*, edited by R. E. Prange and S. M. Girvin (Springer, New York, 1987).
[7] Experiments on tunneling spectroscopy of edge states do not fully agree with the theory either; see a recent review by A. M. Chang, Rev. Mod. Phys. **75**, 1449 (2003).
[8] M. Büttiker, Phys. Rev. Lett. **57**, 1761 (1986).
[9] X.-G. Wen, *Quantum Field Theory of Many-Body Systems* (Oxford University Press, Oxford, 2004).
[10] A. E. Hansen *et al.*, Phys. Rev. B **64**, 045327 (2001).
[11] G. Seelig and M. Büttiker, Phys. Rev. B **64**, 245313 (2001).
[12] F. Marquardt and C. Bruder, Phys. Rev. Lett. **92**, 056805 (2004); Phys. Rev. B **70**, 125305 (2004).
[13] V. S.-W. Chung, P. Samuelsson, and M. Büttiker, Phys. Rev. B **72**, 125320 (2005).
[14] I. Neder *et al.*, arXiv:cond-mat/0610634; I. Neder and F. Marquardt, arXiv:cond-mat/0611372.
[15] In Fig. 1 of Ref. [3] the counterpropagating edge state goes from the source S3 to QPC0 and under the air bridge comes very close to the upper arm of the interferometer, which is the part of the channel between QPC1 and QPC2.
[16] Th. Giamarchi, *Quantum Physics in One Dimension* (Oxford University Press, Oxford, 2003).
[17] J. T. Chalker (unpublished).
[18] We believe that the physics we discuss is not determined by generally complex microscopic properties of QPCs.
[19] Since in our model the interaction is localized inside the interferometer, the perturbation theory in tunneling is free from infrared divergences [16].